Aquifer heterogeneity – is it properly assessed by wellbore samples and does it matter for aquifer heat extraction?

Peter Leary*, Peter Malin, Eylon Shalev & Stephen Onacha
Institute of Earth Sciences and Engineering, University of Auckland
58 Symonds Street, Auckland 1142, New Zealand
p.leary@auckland.ac.nz

Abstract

Oil field reservoir formations are sampled for porosity and permeability on the tacit assumption that small scale well-log and well-core data are representative of the formation flow properties at arbitrary distances from the wellbore. In formal terms, this statistical assumption is valid only if the formation properties are adequately characterised by a mean and standard deviation, or, equivalently, if variations in formation properties are spatially uncorrelated on all scale lengths. This statistical validity condition is, however, violated by crustal rock; well-log and well-core data are spatially correlated over a wide range of scale lengths. It is, therefore, formally wrong to assume that small scale sample means and standard deviations adequately represent large-scale variation of aquifer reservoir/formation properties.

As a practical matter, the formal failure of oil field well-log and well-core sampling to adequately estimate large-scale formation flow property variation is buffered by (i) the high energy density of hydrocarbons, (ii) lack of need for large drainage flow rates, (iii) ability to drill infill wells if *de facto* well drainage volumes are too small, and (iv) ability of time-lapse seismic imaging to detect fluid substitution volumes to determine large-scale formation flow structures that are not inferred from small-scale formation sampling strategies.

As an equally practical matter, however, the above caveats do not apply to producing hot aquifer fluids: (i) geothermal energy density is far smaller than hydrocarbon energy content; (ii) high flow rates are essential to geothermal power production; (iii) infill wells are at high risk to not intersect large drainage volumes unless guided by reliable auxiliary information; (iv) time-lapse hot aquifer imaging has no fluid-substitution signal.

An alternative strategy to aquifer production well-siting based on small-scale wellbore sampling of the aquifer focuses on measuring large-scale aquifer fracture-structures. Experience with magnetotelluric (MT) detection of *in situ* fracture volumes in geothermal fields suggests that MT surveys can form the basis for physically accurate sampling of large-scale aquifer fracture/flow structure.

Keywords: fractures, faults, porosity, permeability

Introduction – Treating aquifers as oil field reservoir formations

The following statement, made at the Bali 2010 World Geothermal Congress, succinctly describes an approach to hot aquifer energy production based on oil/gas reservoir formation characterisation using wellbore samples.

As part of the drilling of the petroleum wells, a significant amount of wireline logging, core sampling and resulting petrophysical evaluation were undertaken…... The porosity of the target ….section was determined…based on wireline logs calibrated to porosity samples from conventional cores and sidewall cores. The core porosities were calibrated to measured permeabilities using all the cores from a larger database…... Several studies…..provide insights into the petrophysical evaluation….and its calibration of porosity to permeability. Using the calibration of porosity to permeability, and the calibrated porosity derived from wireline logging and cores, it is thus possible to determine the permeability….sandstone section and integrate this across the borehole to get the transmissivity or permeability metres. (de Graaf et al 2010).

Parallel statements were made at the WGC2010 by Clauser et al (2010) and Vogt et al (2010). The working assumption is that formation wellbore data recorded by geophysical logging tools and/or recovered in well core adequately samples the formation properties at all relevant scales. While indisputably the wellbore data sample specific geological formations, it does not follow that within a geological formation any or all important geophysical properties conform to a small-scale sample mean throughout the formation, or that important geophysical property variations within the formation are confined to the formation. Rather the evidence from well-log data systematics is precisely the opposite: variation of geophysical properties within a formation can be substantial and these variations can be connected to the enclosing crustal volumes outside the formation. Well-log systematics thus indicate that near-wellbore samples do not accurately assess the degree of large-scale spatial variation expected for *in situ* formation properties, and that the spatial distributions of formation variations cannot be adequately estimated from small-scale sampling.

These general statements are illustrated by well-log and well-core data for Perth Basin formations encountered by the 3km-deep Cockburn1 well.

Well-log and well-core sample data for Perth Basin sedimentary formations

Perth Basin formations were drilled, logged and core-sampled by the 3km-deep Cockburn1 oil exploration well on the coast 18km southwest of Perth (Smith 1967). Well-log data in general, and for the 1200m thick Yarragadee aquifer in particular, conform to well-log *in situ* geophysical property variations observed worldwide. Figure 1 shows the well-log systematics for specific aquifer formations in the Cockburn1 well sequence.

Well-log power-law scaling systematics

The Fourier power-spectra of *in situ* spatial variations of rock properties measured by well logs worldwide closely conform to a specific power-law scaling form (Leary 2002):

$$S(k) \propto 1/k^1, \qquad (1)$$

where k is spatial frequency and S is the well-log fluctuation power at scale length k. Depending upon the well log, the spectral scale-length range k tends to ~3 decades in the overall 5-decade scale range ~1cycle/cm to ~1cycle/km. High spatial frequency data at ~1cycle/cm are recorded by formation microscanner tools measuring electric resistivity with mm-scale electrodes. Km-long well logs of gamma activity, acoustic velocity, neutron density, electron density and electrical resistivity logs routinely return low spatial fluctuation power data at ~1cycle/km.

Well-log spectral form (1) is important for three reasons:

- It is power-law over all scale lengths relevant to reservoir performance and crustal deformation processes;
- The power-law exponent is the same for essentially all *in situ* properties, rock types, and geological settings;
- The non-zero power-law exponent destroys the basis for standard statistical inferences from standard sampling.

Power-law scaling of well-log spatial fluctuations over the five-decade cm-km scale range is indisputable evidence that something beyond geology is at work in the brittle crust. A power-law scaling exponent that is essentially the same for a range of geologic media and settings is evidence that power-law scaling derives from fundamental physical properties of rock with secondary regard to geological details at all scale lengths. Spatially fluctuating grain-scale fracture density is a likely candidate for the fundamental parameter controlling how *in situ* physical properties of rock vary both vertically and horizontally (Leary 2002).

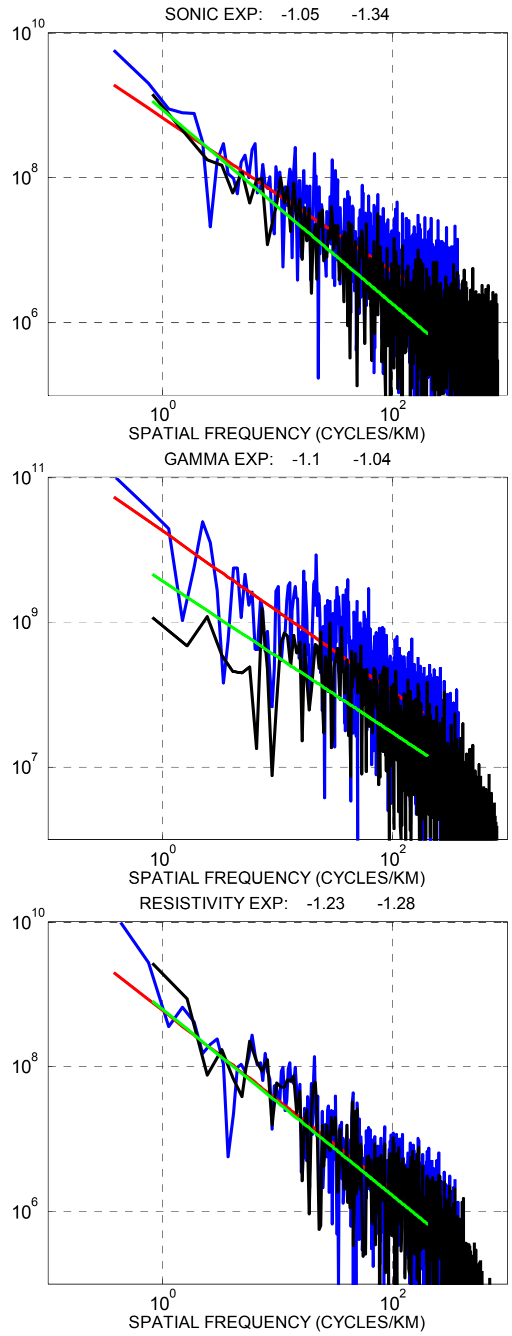

Figure 1: Well-log fluctuation power-spectra for Cockburn1 geological section (blue) and Yarragadee formation (black) fit to power-law trends for sonic velocity, gamma activity and resistivity data. Red line fit to entire section, green line to Yarragadee section. Spectral exponent ~1.17 ± 0.13 is non-zero, showing that fluctuations of *in situ* rock physical properties of the Cockburn1 drill site and the Yarragadee aquifer in particular are spatially correlated rather than spatially uncorrelated over the m-km scale range.

The non-zero power-law scaling exponent in (1) means that *in situ* spatial fluctuations in geophysical properties are spatially correlated at all scale lengths and hence systematically violate the necessary condition of the central-limit theorem upon which standard geostatistical inferences are commonly based.

The general idea that small-scale sample means and standard deviations reasonably represent large-scale property variations within an ensemble is valid only if the ensemble property variations are spatially uncorrelated. Fluctuations are, in turn, uncorrelated only if the associated fluctuation power-law spectrum is 'white',

$$S(k) \propto 1/k^0 \sim constant, \qquad (2)$$

at all relevant scale lengths. Figure 1 tests fluctuation power condition (2) for well-log acoustic velocity, gamma activity, and electrical resistivity data over the entire Cockburn1 section (blue) and the Yarragadee formation (black). Since the power-law exponent of each spectrum is ~1 instead of 0 over the 3 decade m-km scale range, condition (2) for spatially uncorrelated fluctuations in the Cockburn1 well geological section is mathematically untenable. Whatever properties of *in situ* rock are responsible for the variations in well-log readings, it cannot be logically maintained that the mean and standard deviation of small-scale sample data accurately predicts the scale of variations in those properties at arbitrary distances from the wellbore.

Well-core poroperm fluctuation systematics – percolation via grain-scale fractures

An underlying connection between *in situ* fractures and $S(k) \propto 1/k$ power-spectra is plausible since spatial variations in gamma activity of soluble radiogenic minerals, acoustic velocity and electrical resistivity are naturally related to spatial variations in fracture density. That is, crustal volumes with a greater number of fractures tend to have greater gamma activity, lower resistivity and lower seismic velocity. However, physically more immediate evidence for spatially variable fracture density is available through the systematics of well-core porosity-permeability (poroperm) spatial fluctuations measured in numerous oil/gas field reservoir formations (Leary & Walter 2008).

Figure 2 graphically illustrates the systematics of poroperm spatial fluctuations for well-core data from tight gas reservoir formations in the Cooper Basin, South Australia. The blue trace tracks variations in well-core porosity φ and the red trace tracks variations in the logarithm of well-core permeability κ as the core sequence moves along the well. The Figure 2 spatial fluctuation relation between porosity φ and logarithm of permeability κ can be written,

$$\delta\varphi \sim \delta\log(\kappa), \qquad (3)$$

where $\delta\varphi$ and $\delta\log(\kappa)$ denote respectively normalised spatial variations in well-core values of porosity and log(permeability) over a well-core sequence.

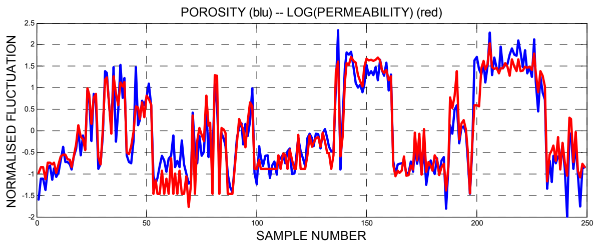

Figure 2: Overlay of poroperm fluctuation data for tight sandstone formations in the Cooper Basin, South Australia. The blue and red traces denote zero-mean/unit-variance fluctuations in, respectively, well-core porosity and the logarithm of well-core permeability. Cross-correlation of the two traces is 85% at zero-lag.

High degrees of spatial cross-correlation (3) are common in the abundant well-core poroperm sequences acquired for clastic reservoir sections.

The cross-correlations have a natural explanation in terms of fluid percolation at grain-scale fractures. Consider a core-sized rock volume of N grain-grain contacts with intact cement bonding and no fluid percolation. Within the core, however, a number $n \ll N$ grain-grain contacts will have cement bonds ruptured by tectonic finite strain deformation, with geofluids able to percolate through the ruptured grain-grain contact. Neighbouring core volumes of N intact grain-grain contacts will vary in their number $n+\delta n$ of ruptured contacts, $\delta n \ll n$.

We know that, say, aquifer rock is permeable to fluids, and (1) tells us that grain-scale fractures probably influence rock properties on scales from cm to km, so it is reasonable to expect that percolation pathways exist across this scale range. We might thus expect that sample rock volumes have porosity variations in proportion to grain-scale density fluctuations, $\delta\varphi \sim \delta n$, while variations in core permeability κ are related to the variation in combinatorial terms $n!$ and $(n+\delta n)!$ that measure the number of ways n and $n+\delta n$ percolation defects can be connected in percolation pathways, $\delta\log(\kappa) \sim \delta\log(n!)$. With this logic, the permeability variation terms evaluate as

$$\delta\log(\kappa) \sim \delta\log(n!) = \log((n+\delta n)!) - \log(n!)$$
$$= \log[((n+\delta n)!)/(n)!)]$$
$$= \log[(n+\delta n)(n+\delta n-1)(n+\delta n-2)\ldots..(n+1)]$$
$$\sim \delta n \log(n).$$

If the defect density n doesn't vary much between well-core samples, and with $\log(n)$ varying much more slowly than n, we can normalise the factor $\log(n)$ out of the above expression to recover the empirical poroperm fluctuation relation (3) in form

$$\delta\log(n!) \sim \delta n. \qquad (4)$$

Thus, if *n* is the number of percolating defects in a unit volume of rock and *n*! is proportional to the percolation permeability of the rock sample with *n* percolation defects, then empirical relation (3) is effectively a mathematical identity, log(*n*!) = *n*(log(*n*) - 1). The close equivalence of (3) and (4) argues that *in situ* permeability is a percolation process in rock volumes whose physical properties on all scale lengths are internally defined by spatially fluctuating populations of grain-scale defects consistent with power-law scaling of well-log spectra (1).

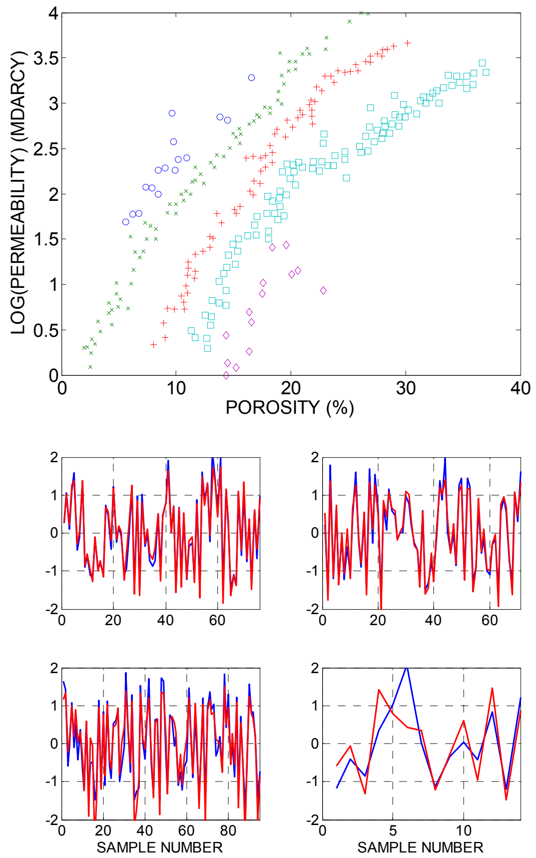

Figure 3: (Upper) Composite poroperm data as traditionally presented in oil and gas literature; a sequence of poroperm traces are sorted by grain size from coarser on left to finer on right. (Lower) Same poroperm data rendered in Figure 2 format; spatial fluctuation correlations between porosity and log(permeability) masked in upper display emerge in agreement with spatial fluctuation relations (3) and (4).

It may be useful to useful at this point to contrast the multi-scale-length spatially-correlated fracture phenomenology of well-log fluctuations (1) and well-core empirical fluctuations (3) and fracture-fluctuation percolation interpretation (4) with the standard treatment of poroperm data in the oil/gas industry literature. With reference to empirical relation (3), the upper plot in Figure 3 shows standard industry presentation of poroperm data for a sequence of size-graded well-core (coarser grain samples on the left grade into finer grain samples on the right). Inherent in this poroperm data presentation is the expectation that each sample is integral into itself, with no reason to suppose that the sample could be systematically related to neighbouring samples on any particular scale length (except, of course, by 'random' happenstance). The lower subplots of Figure 3 show, however, that latent in the poroperm data is the empirical poroperm spatial correlation (3). The subplots render four of the five upper-plot grain-size-graded poroperm data trends in the zero-mean/unit-variance sequence normalisation format of Figure 2. Spatial correlation (3) between porosity and log(permeability) emerges directly from the obscurity of the standard poroperm data presentation.

Again in line with the industry assumption that rock samples are only 'randomly' related to their neighbours, common oil industry practice uses a generic permeability dependence on porosity such as the Carman-Kozeny cubic expression (e.g., Dvorkin 2009; Cox et al 2001; Mavko & Nur 1997),

$$\kappa \sim \varphi^3. \qquad (5)$$

Poroperm dependency (5) is derived from estimates of tubular flow through clusters of pore space without reference to grain-scale fractures or fracture connectivity at any scale. Such formulations with reference only to the smallest scale lengths are consistent with spatially uncorrelated rock property heterogeneity (2) but, of course, make no contact with the essentially universal well-log observation (1) that *in situ* rock property heterogeneity is spatially correlated over five decades of scale length.

Well-log and well-core data thus provide clear lines of evidence that

1. small-scale (wellbore) sampling of permeability does not accurately assess large scale *in situ* permeability variability;
2. *in situ* fractures and fracture-controlled permeability on all scale lengths are an essential ingredient of crustal rock heterogeneity;
3. large amplitude *in situ* permeability heterogeneity is expected at large scale lengths.

Yarragadee well-core poroperm fluctuations

Applying the above argument to the Cockburn1 well data, Figure 4 shows the poroperm spatial fluctuation data for the complete Cockburn1 well-core suite in the Figure 2 format. Dotted data points in Figure 4 mark poroperm data for the Yarragadee aquifer within the Cockburn1 well sequence. In contrast with typical oil field reservoir well-core sample data tightly confined to short intervals of oil-bearing sands, many of the Cockburn1 well-core samples were taken at 100m to 200m intervals over which formation properties change significantly.

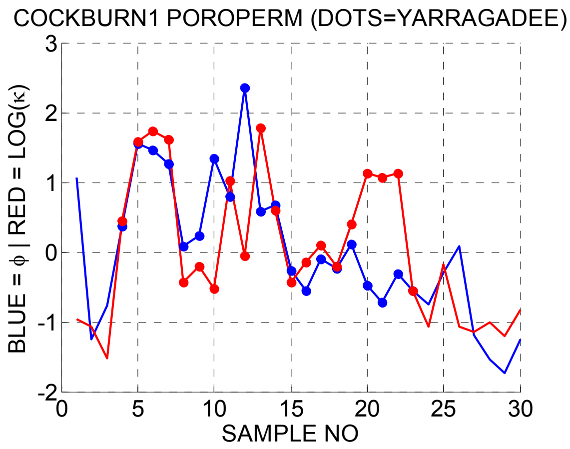

Figure 4: Cockburn1 well-core poroperm data sequence in Figure 2 format (blue = porosity, red = log(permeability) normalised to zero-mean/unit-variance). Compared with standard oil field reservoir poroperm fluctuations in, say, Figure 2, departures from close spatial correlation are due to well-core samples being taken at 100m intervals in varying formations.

Despite the far more variable nature of the Cockburn1 well rock-type and formation-type poroperm sampling, Figure 5 shows 60% zero-lag spatial correlation (red trace) between variations in Cockburn1-well sample porosity and sample log(permeability). The blue trace indicates the typical 20% level of cross-correlation excursion of spatially-uncorrelated fluctuation sequences with spectral content of the Cockburn1 poroperm data. The 60% Cockburn1 data cross-correlation peak at zero-lag is statistically significant.

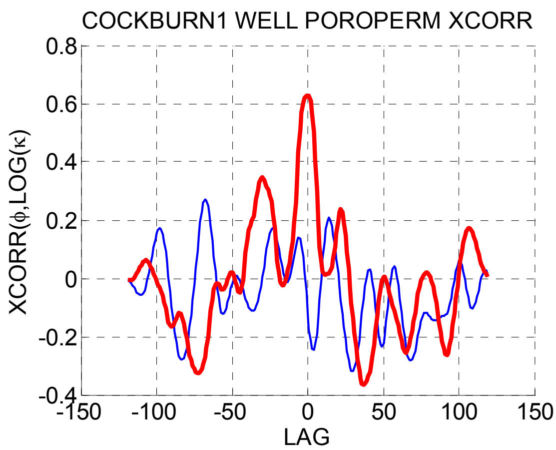

Figure 5: (Red) Cross-correlation of resampled Cockburn1 well-core poroperm data sequences. (Blue) Cross-correlation of uncorrelated random sequences with frequency content of well-core poroperm data; 60% correlation between poroperm sequences at a specific lag (here zero) is seen to be statistically significant.

Fracture heterogeneity and hot aquifer energy production

The foregoing discussion challenges the oil/gas industry reservoir characterisation assumption that spatially sparse wellbore samples more or less represent geological formation properties at all larger scale lengths. Plentiful well-log and well-core data instead point to *in situ* percolation flow processes controlled by spatially-correlated random fracture networks on all scale lengths. Such random fracture networks are spatially erratic and effectively unpredictable from small-scale sparse sampling, leading to a degree of geofluid flow spatial heterogeneity consistent with the statistics of production well drilling success.
The following quote assesses the success rate of drilling geothermal wells at one half the success rate of drilling oil/gas wildcat wells:

Given the extremely high degree of uncertainty involved in well siting and design, hydrothermal exploration success rates are around 25%, estimates the GEA. That compares with a worldwide oil wildcat success rate of 45% in 2003, according to IHS Energy, a consultancy. (Petroleum Economist 2009),

While a number of factors affect both production well success/failure rates, two factors stand out:

- oil and gas are far more energy rich than hot water;
- to be profitable oil and gas do not have to come of out the ground at high flow rates but hot water does.

With the chemical energy of oil about 50MJ per litre, and long-term oil field production average rate ~1 litre per 4 seconds (~15 barrels of oil per day for ~5×10^5 US wells for years 1954-2006, www.eia.doe.gov/aer/txt/ptb0502.html), wellhead power production for a typical oil well is of order 12MW. In contrast, a geothermal well discharging N litres per second of water with $\Delta T^{o}C$ excess temperature produces about $4\text{x}N\text{x}\Delta T/1000$ MW of thermal power. For $\Delta T = 100^{o}C$, it requires N ~ 25 litre/s to produce 10MW of thermal power. For equal wellhead power production, a geothermal well flow rate must thus be of order 100 greater than an oil well.
Translating geofluid flow rate into dollar-rate to cover drilling costs, and taking into account the different efficiencies of electrical power production, a geothermal well must flow on order 300 times greater rate to produce an income equivalent to pure oil recovery. Allowing for production of water as well as oil, 90% water cut requires a geothermal well to flow effectively 30 times the rate of its oil equivalent for comparable income to cover drilling costs.

These contrasting order-of-magnitude well-flow-rate numbers for hydrocarbon and geothermal power production make it clear that effective geothermal production well siting demands understanding the potential for flow heterogeneity of the target formation. It is not surprising that the global success rate for geothermal production well success is one half that of hydrocarbon wildcat wells. Within a developed hydrocarbon reservoir, the rate of infill drilling success is probably substantially higher than wildcat well success, giving all the more reason to be cautious about adopting oil field practices regarding aquifer permeability distributions.

To make aquifer energy production commercially viable, physical logic and practical experience indicate that close attention needs to be paid to finding aquifer volumes of sufficient size and fracture density that production wells can cover their cost. To that end, we discuss several surveys of producing geothermal fields in which:

- MT data identified reservoir volumes of significant aligned fracture density;
- production wells drilled in the MT-identified aligned-fracture reservoir volumes had flow rates far exceeding the field average.

An MT approach to sounding for large-scale aquifer fracture structures

Magnetotellurics (MT) is the practice of measuring the natural magnetic field fluctuations of the earth's atmosphere as they reach the earth's surface, and at the same time and place measuring electric (telluric) currents induced by the travelling magnetic fields. By measuring the natural magnetic and induced electric fields over a wide range of temporal frequencies (as high as 1-10kHz to as low as 0.1mHz), the electrical conductivity of the earth at a specific site can be inferred as a function of electromagnetic wave depth penetration.

An important aspect of MT data is that the measurements can register systematic a amplitude differences in electrical currents running along fracture trends versus electrical currents running across fracture trends. Since currents move more easily along fracture trends, the earth appears more conductive (less resistive) along fracture trends, and less conductive (more resistive) across fracture trends. MT surveys, thus, are sensitive to a dual phenomenology closely relevant to fluids and fractures:

- over a range of (x,y) coordinates a sequences of MT stations can seek out zones in which electrical currents flow better in one direction than they do in the orthogonal direction;
- the same MT data can reveal the approximate depth to the current-flow directional anomalies by noting at which MT field frequencies the anomalies first occur.

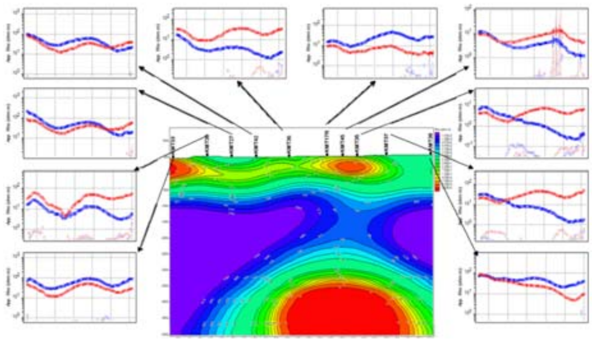

Figure 6: Summary of 5km MT traverse of Krafla, Iceland, geothermal field. Central figure is deduced resistivity profile beneath the survey traverse. Peripheral plots are resistivity depth profile data in the form of measured MT field resistivity versus MT field wavelength. Red curves denote data for electric currents along the traverse, blue curves data for electric currents across the traverse. Left ends of resistivity curves are for shorter wavelengths (shallower depths), right ends for longer wavelengths (deeper depths). Divergence of blue/red curves interpreted as evidence that current-carrying aligned fractures run in/out of the section plane, with fractures concentrated in the volume denoted by the red oval at the base of the crustal section.

Figures 6-7 illustrate the dual phenomenology of fracture-related MT surveys over a 5km crustal volume enclosing the Krafla geothermal field of central Iceland (Malin et al 2009; Onacha et al 2010). The Krafla field sits astride the NE-SW-trending mid-Atlantic rift system as it passes through central Iceland. Figures 6-7 show that the geothermal activity along the rift system is greatest where a shallow NW-SE trending tectonic fault system intersects the NE-SW rift trend.

The MT surveyed Krafla crustal volume partitions into more resistive rock represented as cold colours and more conductive rock represented as warm colours. MT surveys across the volume return paired sequences of resistivity versus depth profile displayed as blue and red curves for each MT station. The red curve measures the resistivity profile parallel to the MT traverse; the blue curve measures resistivity normal to the traverse.

Figure 6 summarises a rift-parallel SW-NW (left-right) MT traverse of the Krafla crustal volume. The leftmost survey station resistivity profile is shown in the lower-left panel. The blue and red MT profile curves do not diverge significantly as MT wavelength increases from left to right (shallow data register at left end of curve, deep data register at right end of curve). A lack of systematic divergence between blue and red resistivity profile curves persists over the next three MT stations moving clockwise from the lower-left panel. When, however, the MT survey moves to the vicinity of the deep conductivity anomaly represented as the red oval at depth in the crustal section, the red and blue resistivity curves begin to diverge with increasing MT signal wavelength. Relative to the electrical current flowing in the plane of the traverse (red curve), the current flow in/out of the traverse plane increases, hence the effective resistivity drops (blue curve). Except for the next station (presumably affected by the near-surface low resistivity red zone), the blue-curve-lower-than-red-curve resistivity profile relation persists through the succeeding four survey stations, thus establishing the existence of the buried red oval high conductivity structure. This structure, given by the blue resistivity profiles, defines a NE-SW trending fracture/fault system intersecting the rift-oriented NE-SW traverse plane.

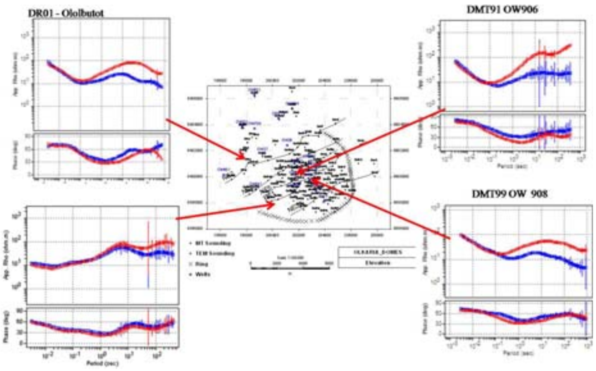

Figure 7: Map MT station resistivity depth profile distribution for the Krafla, Iceland, geothermal field as in Figure 6. The upper-left and right-hand resistivity profiles show that electrical currents travelling NW-SW are strong along the MT station sequence line, while the lower-left resistivity profile shows that away from the NW-SE line the NW-SE electrical currents are reduced. By inference, the 3-station line locates a local fracture/frault trend; in the Krafla geothermal field this line collocates with a known tectonic fracture trend.

Figure 7 displays the Figure 6 resistivity phenomenology for a map distribution of MT stations. The NW-SE trend of 3 upper-left + right-hand resistivity profile panels defines the fracture trend seen as the red high-conductivity feature at depth in Figure 6. For each of the 3 MT stations, the blue resistivity curve diverges strongly from the red curve, indicating enhanced ability to carry current along the NW-SE trend. In contrast, the lower-left MT station sees significantly smaller resistivity profile divergence, implying that at depth at this location there is much reduced fracture alignment to carry electrical currents at depth. Geologically, the 3-station NW-SE MT station trend in Figure 7 collocates with a known regional fault system normal to the NE-SW trending rift system.

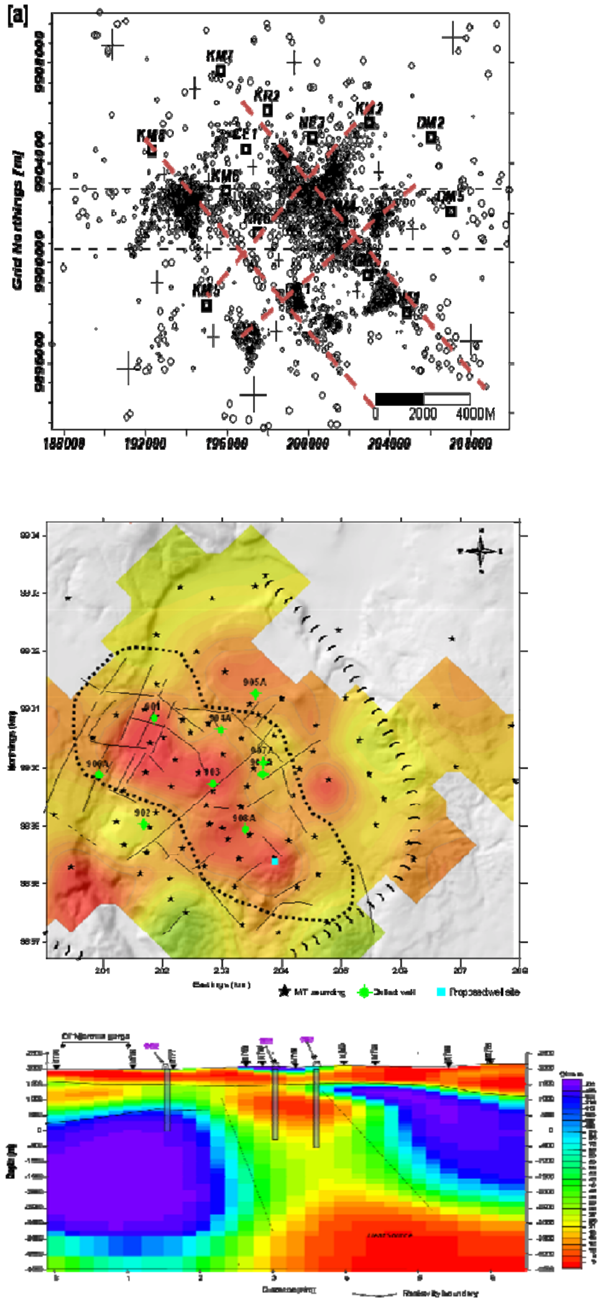

Figure 8: (Upper) Seismicity at the Olkaria, Kenya, geothermal field; the NE-SW trends lie along the East Africa Rift; the NW-SE trends lie along a local tectonic fault feature; (centre) MT resistivity distribution summary in which red/yellow tints denote areas of high/low electrical conductivity for the NW-SE aligned fractures; (lower) production well history along NE-SW rift trend, with lefthand well in yellow tint zone a poor producer and righthand wells in red tint zone well above average producers.

The three parts of Figure 8 summarise a similar fault-intersection phenomenology observed in the Olkaria, Kenya, East Aftrica rift system geothermal field (Simiyu & Malin 2000; Onacha et al 2009). The upper plot of Figure 8 seismically defines two fault trends, the NE-SW trend along the rift, and the NW-SE trend along a locally defined tectonic fault. The centre plot is a composite rendering of MT survey data in which red tints mark MT sites for which NW-SE rift-normal electrical currents are strong while yellow tints mark MT sites where such electrical currents are weak. The lower plot summarises the production well history: the lefthand well drilled in the yellow-tinted MT zone is a poor producer, while the two righthand wells drilled in the red-tinted MT zone produce at double to triple the field average production rate.

Summary/Conclusions

We argue:

- well-log and well-core systematics show that fracture systems are important, perhaps (probably?) crucial, conduits for geofluid flow on all scales in all rock, with particular reference to aquifer rock currently targeted for heat extraction;
- power-law scaling well-log spectra indicate that small-scale rock samples fundamentally do not represent the range of rock property fluctuations likely to occur at large scale lengths;
- in absence of utility from small-scale sampling of rock properties, and in light of essentially unlimited fluctuations in rock properties on large scales, it is logical to consider large scale sampling of rock formations for information on *in situ* permeability;
- large scale measurements of fracture distributions are particularly relevant where geofluid flow rates are essential to drill hole success;
- in geothermal fields, where fractures are almost universally acknowledged to control geofluid flow, MT resistivity profiles indicate that geofluid flow is greatest where known fracture/fault trends intersect; enhanced production well flow has validated MT data as a geophysical guide to well siting.

We conclude from these arguments that MT surveys of potentially exploitable hot aquifers are a plausible investment in advance of costly drilling.

References

Clauser C, Marquart G, Rath V & MeProRisk Working Group (2010) MeProRisk – a Tool Box for Evaluating and Reducing Risks in Exploration, Development, and Operation of Geothermal Reservoirs, World Geothermal Congress, Bali April25-30 2010.

Crude Oil Production and Crude Oil Well Productivity, 1954-2008 www.eia.doe.gov/aer/txt/ptb0502.html

de Graaf L, Palmer R & Reid I (2010) The Limestone Coast Geothermal Project, South Australia: a Unique Hot Sedimentary Aquifer Development, World Geothermal Congress, Bali April25-30 2010.

Dvorkin J (2009) Kozeny-Carman equation revisited, pangea.stanford.edu/~jack/KC_2009_JD.pdf

Leary P (2002) Fractures and physical heterogeneity in crustal rock, in Heterogeneity of the Crust and Upper Mantle – Nature, Scaling and Seismic Properties, J. A. Goff, & K. Holliger (eds.), Kluwer Academic/Plenum Publishers, New York, 155-186.

Leary PC & Walter LA (2008) Crosswell seismic applications to highly heterogeneous tight-gas reservoirs, Special Topic on Tight Gas, First Break 26, 33-39.

Malin P, Leary P, Shalev E & Onacha S (2009) Joint Geophysical Imaging of Poroperm Distributions in Fractured Reservoirs, GRC *Transactions*, Vol. 33, 4-7October 2009

Mavko, G., and Nur, A., 1997, The effect of a percolation threshold in the Kozeny-Carman relation, Geophysics 62, 1480-1482.

Onacha S, Shalev E, Malin P, & Leary P (2009) Joint Geophysical Imaging of Fluid-Filled Fracture Zones in Geothermal Fields in the Kenya Rift Valley, GRC *Transactions* Vol. 33, 4-7October 2009

Onacha S, Shalev E, Malin P, Leary P & Bookman L (2010) Interpreted Fracture Anomalies: Joint Imaging of Geophysical Signals from Fluid-Filled Fracture Zones in Geothermal Fields, Proceedings World Geothermal Congress, Bali, Indonesia, 25-29April 2010

Petroleum Economist (2009) Unlocking the value of the world's geothermal resources, www.petroleum-economist.com

Simiyu S & Malin P (2000) A "volcano seismic" approach to geothermal exploration and reservoir monitoring: Olkaria, Kenya and Casa Diablo, U.S.A. World Geothermal Congress 2000, Kyoto-Tohoku Japan, 1759-1763.

Smith DN (1967) Well Completion Report Cockburn No. 1 Well, Western Australia, West Australian Petroleum Pty. Ltd

Vogt C, Mottaghy D, Rath V, Wolf A, Pechnig R & Clauser C (2010) Quantifying Uncertainty in Geothermal Reservoir Modeling, World Geothermal Congress, Bali April25-30 2010.